Investigation of Non-Newtonian Flow Behavior in Oldroyd-B Ternary Nanofluid: Analyzing the Thermal Efficiency of Solar Radiation on Water Pumping Systems

A. M Obalalu[1], *Ephesus O.* Fatunmbi[2], *Abhijit Singh* Bhakuni[3], *Mohit* Bajaj[4,5*], *A. M.* Abdul-Yekeen[6], *O. B* Ojewola[7]

[1] Department of Mathematics and Statistics, Kwara State University, Malete, Nigeria
[2] Department of Mathematics and Statistics, Federal Polytechnic, Ilaro, Nigeria
[3] Department of ECE, Graphic Era Hill University, Bhimtal, Uttarakhand, India
[4] Department of Electrical Engineering, Graphic Era (Deemed to be University), Dehradun-248002, India
[5] Graphic Era Hill University, Dehradun, 248002, India
[6] Lamar University Beaumont Texas, USA
[7] Department of Pure and Applied Mathematics, LAUTECH, Ogbomosho, Oyo State, Nigeria

Abstract. Solar water pump plays an important role in utilizing renewable energy for several purposes, such as irrigation farming, community water supply and livestock watering. Regardless of the positive influence they have on the environment, these systems often experience difficult related to energy inefficiency. Therefore, the main prospective of this research to tackle this difficulty by investigating the potential of Oldroyd-B Ternary nanofluid to increase the heat transport efficiency and performance of SWP systems. The Ternary nanofluid consists of Silicon Dioxide (SiO_2), Silver (Ag), Copper (Cu) nanoparticles suspended in Water (H_2O). Also, the employment of O-BHNF flowing in parabolic trough surface collector (PTSC) used inside SWP has been developed to evaluate thermal efficacy The wavelets and the Chebyshev Wavelet method is utilized to compute the numerical solutions. The outcome indicate that the temperature distribution boosted as the solar radiation parameter increases. The mixture of $SiO_2 + Ag + Cu/H_2O$ ternary nanofluid leads to high thermal radiative performance compared to hybrid with $Ag + Cu/H_2O$.
Keywords. Ternary nanofluid; solar radiation; non-Newtonianism Oldroyd-B; solar water pump.

1 Introduction

The complex nature of non-Newtonian fluids has necessitated the formulation of several models, each capturing specific properties of the non-Newtonian fluid characteristics, [1-2]. However, their enormous applications in various fields of human endeavour, such as food processing, oil drilling, chemical engineering, and biomedical engineering, among others, have inspired researchers to pay more attention to their studies, [3-4]. The viscosity of non-Newtonian fluids exhibits various characteristics, including shear thinning, shear thickening, viscoelastic, thixotropic, Bingham plastics, and rheopectic. The viscoelastic fluids display both viscous and elastic characteristics. These fluids have a viscous property that allows them to flow like liquids while simultaneously exhibiting elastic behaviour that allows them to return to their original shape after deformation. Their molecular properties enable them to display these dual properties. One prominent member of the viscoelastic fluid model is the Oldroyd-B model, which possesses a non-constant viscosity and exhibits a time-dependent character with a complicated stress-strain relationship [4-6]. In this model, the stress is dependent on the present and former positions of strain and strain rate. It describes a complex and sophisticated model that is valuable in many engineering and manufacturing processes, including polymer engineering, paint and printing rheology, and bio-medical engineering. Typical examples include melts and polymer solutions, blood, and other biological fluids [7-8]. In their study, Shezhad et al. [9] applied HAM to tackle this type of fluid model configured in a laterally extending 3D plate with variable thermal conductivity and a heat source or sink. Dadheech et al. [10] investigated a numerical model of Oldroyd-B fluid moving over a permeable plate with slip conditions, melting properties, and a magnetic effect. Hamza [11] discussed the flow dynamics of such a model in a porous circular channel with magnetic field effects and a time-

*Corresponding author: thebestbajaj@gmail.com

dependent pressure gradient. Song et al. [12] employed an analytical tool via integral transform to evaluate the transport of such a model in a fluctuating rectangular duct. Tiwana et al. [13] applied the Laplace method to discuss the transient flow of the Oldroyd-B fluid in a vertical porous enclosure featuring a ramped surface temperature. However, the efficiency of this fluid model can be further enhanced in the presence of nanoparticles.

Over the years, researchers and scientists have been concerned about the poor thermal heat transfer performance of traditional fluids. This concern stems from advancements in science, technology, and engineering activities that require fluids to improve heat transfer in various thermal engines and devices. In many fields, such as transportation industries, electronic cooling systems, pharmaceuticals, and so on, improving heat transmission has become a major requirement. However, ordinary fluids such as oil, water, ethylene, or propylene glycol could not provide the necessary heat transfer. As a result, Choi [14] pioneered the class of fluids called nanofluids. This class of fluids originated from the suspension of tiny nanoparticles ranging from 1–100 nm in a base fluid to boost the thermophysical attributes of ordinary fluids. As a result, the fluid's thermal conductivity increases, resulting in enhanced heat transfer characteristics for the nanofluid. This discovery and its applications prompted many researchers to devote time and energy to studying nanofluids, as contained in Refs [15-19]. The quest to raise the thermal properties of traditional and nanofluids has given birth to hybrid nanofluids. The addition of two distinct nanoparticles to traditional fluids led to the emergence of this new class, which aims to enhance heat transfer. The hybridized nanofluids have more surface area, better dispersion stability with random movement of the tiny particles, and better thermal conduction with heat transfer compared to mono nanofluid and regular fluids. The hybridization of nanoparticles are useful in a variety of applications, including thermal energy control, heat exchangers, solar energy, air conditioning applications, coolant in machining and manufacturing, nuclear and electronic cooling systems, agricultural equipment, chemical machines, and automobile industries [20]. In light of these essential applications, many authors have examined the dynamics of flow and thermal characteristics of hybrid nanofluids in diverse configurations featuring different parameters of interest and boundary conditions. Fig 1 displays the capturing energy with nanotechnology. Scott et al. [21] discussed a comprehensive technological review of hybrid nanofluids and affirmed the superiority of the hybrid nanofluids over mono nanofluids and convectional fluids in terms of heat transfer enhancement. Qureshi et al. [22] conducted an analysis to discuss the heat transmission of a hybridized fluid containing nanoparticles using water as a coolant. They built their numerical model on a rectangular plate, incorporating thermal radiation and the combined effects of porosity and magnetic field. Yunis et al. [23] analyzed a water-based and ethylene glycol-based hybridized nanofluid using the photovoltaic thermal system. The authors reported that the efficiency of energy and exergy increased by 4.1% and 4.6%, respectively. Verma et al. [24] experimentally discussed the significance of hybridized nanofluids containing a horizontal solar collector. In their research, the authors compared the energy and energy ratio efficiency with that of a mono nanofluid, and they reported that the thermal efficiencies of the various combinations of the hybridized fluids were 18.05% and 20.52%.

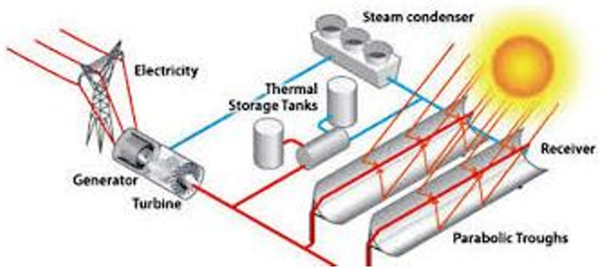

Figure 1. Capturing Energy with Nanotechnology

A recent innovation in the nanotechnology is the dispersion of three distinct nanoparticles in a base fluid, this innovation is termed ternary hybrid nanofluid. This development has been found to be of higher thermal conductivity and produces enhanced heat transfer than the suspension of two kinds of nanoparticles in a base fluid. In view of this implication, Adnan et al. [25] developed a mathematical model for flow dynamics of a ternary hybridized fluid which comprises three distinct nanoparticles of $Al_2O_3 - CuO - Fe_3O_4/C_2H_6O_2$ over a channel with slip and dissipative properties. A discussion of the impact of combined nanoparticles of Copper (II) Oxide, Magnesium Oxide, and Titanium oxide forming H_2O based ternary nanofluid was offered by Mousavi et al. [26]. The computational analysis revealed that the thermal conduction of the ternary hybridized nanofluid increased the with a rise in the volume fraction. Elnaqeeb et al. [27] discussed the importance of surface mass flux in the flow dynamics of a ternary hybridized nanofluid over a 3D plate that stretched bilaterally subject different shapes and densities. Wenhao et al. [28] employed the shooting method to scrutinize joint effects of natural and mixed convection motion of a water-based ternary nanofluid flow having nanoparticles shapes of spherical carbon nanotubes, cylindrical graphene, and platelet. Oke et al. [29] assessed an MHD ternary hybrid nanofluid containing $CNTs$, graphene and alumina over 3D plate experiencing rotation, slip and suction properties. The numerical computation disclosed that the velocity profiles depreciate with a rise in the stretching term along x axis, but the trend was changed in y direction. The use of solar energy as an alternative means of energy that prevents the emissions of CO_2 which post danger to human life has been recently discussed among some researchers.

The recent development in supply of clean energy free from CO_2 emissions has shown that solar energy is significant for use in the industries and in the domestic's activities. This source of energy comes from the sun and has the capacity to produce electricity that is free from CO_2 and thus, contributes to preserving human environment, [30-31]. Different from fossil fuels, it offers a cleaner mechanism to provide the needed energy without negatively impacting on the planet earth. The recent energy demand to meet the advancement in technology without adverse effect on human life, solar energy has become a sought after in many societies. As found in the literature, the solar energy is categorized into two types: the photovoltaic and the concentrated solar power, [32]. The first category involves using semiconductors to convert the energy from the sun into electrical power. The photovoltaic cells are made of silicon and have the capacity to release electrons when exposed to the sun rays, consequently, current electricity is being induced, [33]. On the other hand, the concentrated solar power uses mirror or lenses to transform solar energy into electricity by focusing on a small surface area. Besides, this kind thus apply diverse means like PV cells, heat engines, etc, to transform solar energy into electricity. The use of solar energy in agriculture cannot be over stressed, for instance, farm machines, water pumps for irrigation, are typical examples. Solar water pumps find usage in agricultural practices all over the world, they are used for the supply of water for irrigation purposes without increasing the greenhouse gas emissions. This mechanism seems to be cost effective, prevents fossil fuels extension, contributes to safe environment and offer an enhanced crop productivity, among other benefits [34-35]. These and many more advantages have caught the attention of many researchers and scientists, and at such devoted time and energy to its study. Obalalu et al. [32] constructed a mathematical model of a non-Newtonian fluid with ethylene glycol-based hybridization of aluminum alloy and titanium alloy nanomaterials over a parabolic trough surface collector for solar water pumps. The model incorporated the entropy analysis and radiative heat flux for the measurement of solar energy water pump. The outcomes of the study revealed that, the Biot number, radiative with heat source term and slip parameter improve heat transmission in the system. Shahzad et al. [36] engaged the Oldroyd-B fluid to explain the solar thermal radiative improvement in the solar water pumping systems in the presence of entropy production. In their work, an engine oil is used as a base fluid for the hybridized Cu and GO nanoparticles subject to varied thermal conductivity, slip properties and heat source effects. The report showed that escalating radiation and varying thermal conduction terms caused an enhancement in the solar water pump system. Other related studies can be found in Refs [37-38]. However, the effective of solar water pumps can be enhanced with the use of ternary hybrid nanofluid. In the presence of parabolic trough solar collector. This insight has not been studied by the previous researchers and thus serve as brilliant idea to be investigated in the current study.

1.1 Modeling purpose

Therefore, the current investigation intends to explore the flow characteristics of Oldroyd-B ternary nanofluid for the thermal efficiency of solar radiation in water pump systems. This study applies a parabolic trough solar collector, a new technology for connecting concentrated solar energy, to enhance the thermal performance of solar water pumps. The uniqueness of this study is the dispersion of three kinds of nanoparticles in a base fluid mixed with the non-Newtonian behaviour of Oldroyd-B fluid for the enhancement of solar thermal radiation for use in water pumping for agricultural purposes. To the best of the authors' knowledge, no previous study has conducted this investigation in its current form in the literature. This study includes various figures and tables to discuss the usefulness of the involved parameters.

2 Mathematical formulations

The explanation of the relevant conceptual foundation and limitations concerning the flow model are presented as follows.

- Water as Base fluid, Boundary-layer estimate, Tiwari–Das model.
- Two-dimensional laminar flow, Silicon Dioxide, Silver, Copper.
- Entropy production, Electromagnetic, Porous medium, solar radiation.
- Solar water pump, slippery boundary condition.

Figure 1 exhibited the Physical model and coordinates system of Solar water pump.

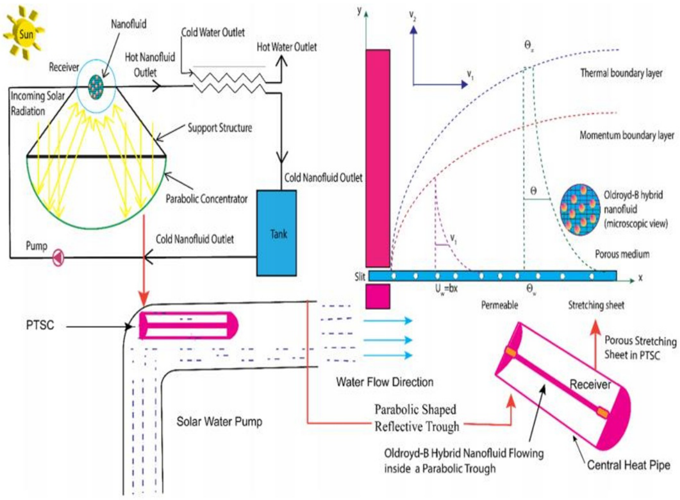

Figure 2: Illustration of present theoretical study.

$$\frac{\partial G_1}{\partial x}+\frac{\partial G_2}{\partial y}=0, \tag{1}$$

$$G_1\frac{\partial G_1}{\partial x}+G_2\frac{\partial G_2}{\partial y}+\gamma_1\left({G_1}^2\frac{\partial^2 G_1}{\partial x^2}+{G_2}^2\frac{\partial^2 G_1}{\partial y^2}+2G_1G_2\frac{\partial^2 G_1}{\partial x\partial y}\right)=\frac{\mu_{thnf}}{\rho_{thnf}}\left(\frac{\partial^2 G_1}{\partial y^2}\right)-\frac{\mu_{thnf}}{\rho_{thnf}}\left(\frac{A_2}{k}\right)+\frac{\mu_{thnf}}{\rho t_{hnf}}\left(\gamma_2\left(G_1\left(\frac{\partial^3 G_1}{\partial x\partial y^2}\right)-\frac{\partial G_1}{\partial x}\left(\frac{\partial^2 G_1}{\partial y^2}\right)+\frac{\partial G_2}{\partial y}\left(\frac{\partial^2 G_1}{\partial y^2}\right)+G_2\left(\frac{\partial^3 G_1}{\partial y^3}\right)\right)\right), \tag{2}$$

$$G_1\frac{\partial \phi}{\partial x}+G_2\frac{\partial \phi}{\partial y}=\frac{k_{thnf}}{\left(\rho C_p\right)_{thnf}}\left(\frac{\partial^2 \phi}{\partial y^2}\right)+ \tag{3}$$

$$+\frac{1}{(\rho C_p)_{thnf}}Q(\phi-\phi_w)+\frac{\mu_{hnf}}{(\rho C_p)_{thnf}}\left(\frac{\partial G_1}{\partial x}\right)^2 -\frac{1}{(\rho C_p)_{thnf}}\left(\frac{\partial q_r}{\partial y}\right)+\frac{\sigma_{hnf}B_0^2}{(\rho C_p)_{thnf}}G_1^2,$$

$$E_G=\frac{k_{nf}}{\phi_\infty^2}\left[\left(\frac{\partial\phi}{\partial y}\right)^2+\frac{16}{3}\frac{\sigma^*\phi_\infty^3}{k^*\upsilon_f(\rho C_p)_f}\left(\frac{\partial\phi}{\partial y}\right)^2\right] \quad (4)$$

Subjected to:

$$G_1(x,0)=U_w+M_w\left(\frac{\partial G_1}{\partial y}\right),\ G_2(x,0)=P_w,\ -k_O\left(\frac{\partial\phi}{\partial y}\right)=h_g(\phi_w-\phi),\ G_1\to 0,\frac{\partial G_1}{\partial y}\to 0,\phi\to\phi_\infty,\text{as}\quad y\to\infty \quad (5)$$

The symbols used in this study are accompanied by information on the thermo-physical properties of the nanofluid, as presented in symbols and expressions section.

2.1. Aspect of Ternary Nanofluid (TNF)

The present work incorporating three kinds of nanoparticles (NPs), specifically Silicon Dioxide (SiO_2), Silver (Ag), Copper (Cu) into Water (H_2O), which served as the base fluid (BF). The NPs were added at varying concentration factors denoted as φ_{SiO_2}, φ_{Ag} and φ_{Ag}. By blending NPs with a base fluid, TNF are established. When this mixture is introduced into a standard fluid, it boosts rate of thermal transport by improving the heat supply capacity. Research conducted in over the past several years has focused on studying the prospective advancement in heat exchanger performance via the utilization of nanomaterials. Scientists have discovered that Silicon Dioxide (SiO_2), Silver (Ag), Copper (Cu) at the nanoscale have the capacity to boost thermal transport efficiency in heat exchangers. Table 1 below shows display the thermo-physical aspect of (TNF).

Table 1: Thermo-physical aspect of (TNF)

Physical property	H_2O	*Cu*	*Ag*	SiO_2
$\rho/(kg.m^{-3})$	997.1	8933	10500	2270
$k/(W.mK)$	0.6071	401.0	429	1.4413
$C_p/(J.kgK)$	1910	385.0	235	730
$\sigma(Sm^{-1})$	5.5×10^{-6}	5.96×10^{7}	6.3×10^{7}	3.5×10^{6}

Thermophysical characteristics of non-Newtonian nanofluid are given as:

$$\mu_{nf}=\frac{\mu_{bf}}{(1-\phi)^{2.5}}, \quad (6)$$

$$\frac{K_{nf}}{k_{bf}}=\frac{(k_{np1}+2k_{bf})-2\phi_1(k_{bf}-k_{np1})}{(k_{np1}+2k_{bf})+\phi_1(k_{bf}-k_{np1})}$$

$$(\rho C_p)_{nf}=(1-\phi_1)(\rho C_p)_{bf}+\phi_1(\rho C_p)_{np1}$$

$$\rho_{nf}=(1-\phi_1)\rho_{bf}+\phi_1\rho_{np1}$$

The thermophysical properties of hybrid nanofluid are given as:

$$\mu_{hnf}=\frac{\mu_{bf}}{(1-\phi_1)^{2.5}(1-\phi_2)^{2.5}}, \quad (7)$$

$$\frac{K_{hnf}}{k_{nf}}=\frac{(k_{np2}+2k_{nf})-2\phi_2(k_{nf}-k_{np2})}{(k_{np2}+2k_{nf})+\phi_2(k_{nf}-k_{np2})}$$

$$(\rho C_p)_{hnf}=(1-\phi_2)(\rho C_p)_{nf}+\phi_2(\rho C_p)_{np2}$$

$$\rho_{hnf}=(1-\phi_2)\rho_{nf}+\phi_2\rho_{np2}$$

$$\frac{\sigma_{hnf}}{\sigma_{nf}}=\frac{(\sigma_{np2}+2\sigma_{nf})-2\phi_2(\sigma_{nf}-\sigma_{np2})}{(\sigma_{np2}+2\sigma_{nf})+\phi_2(\sigma_{nf}-\sigma_{np2})}$$

The thermophysical properties of Tri-hybrid nanofluid are given as:

$$\mu_{Trihnf}=\frac{\mu_{bf}}{(1-\phi_1)^{2.5}(1-\phi_2)^{2.5}(1-\phi_3)^{2.5}}, \quad (8)$$

$$\frac{K_{Trihnf}}{k_{hnf}}=\frac{(k_{np3}+2k_{hnf})-2\phi_3(k_{hnf}-k_{np3})}{(k_{np3}+2k_{hnf})+\phi_3(k_{hnf}-k_{np3})}$$

$$(\rho C_p)_{Trihnf}=(1-\phi_3)(\rho C_p)_{hnf}+\phi_3(\rho C_p)_{np3}$$

$$\rho_{Trihnf}=(1-\phi_3)\rho_{hnf}+\phi_3\rho_{np3}$$

$$\frac{\sigma_{Trihnf}}{\sigma_{hnf}}=\frac{(\sigma_{np3}+2\sigma_{hnf})-2\phi_3(\sigma_{hnf}-\sigma_{np3})}{(\sigma_{np3}+2\sigma_{hnf})+\phi_3(\sigma_{hnf}-\sigma_{np3})}$$

2.2. Transformation analysis

The boundary value problem, including equations 1 to 4, has been transformed into ordinary differential equations following the application of the similarity method.

$$G_1=\frac{\partial\psi}{\partial y},\ \text{and}\ G_2=-\frac{\partial\psi}{\partial x},\ \Gamma(x,y)=\sqrt{\frac{b}{\upsilon_f(1-\Gamma t)}}y,\theta(\Gamma)=\frac{\phi-\phi_\infty}{\phi-\phi_\infty},\ \psi(x,y)=\sqrt{\frac{\upsilon_f b}{(1-\Gamma t),}}xf(\Gamma) \quad (9)$$

By utilizing above equation, we obtain.

$$f'''(\Gamma)+\chi_a\chi_b(ff''(\Gamma)-f'^2(\Gamma))-\frac{1}{\omega_1}K_nf'(\Gamma)+\chi_a\chi_a(2\beta_1 f(\Gamma)f'(\Gamma))+\beta_2 f''^2(\Gamma)+\chi_a\chi_b(\beta_1 f^2(\Gamma)f'''(\Gamma))-\beta_2 f(\Gamma)f''^{v}(\Gamma)=0, \quad (10)$$

$$\theta''(\Gamma)\left(1+\frac{1}{\chi_d}RdPr\right)+\frac{\chi_a}{\chi_b}Prf(\Gamma)\theta'(\Gamma)-\frac{\chi_c}{\chi_a}P_rf(\Gamma)\theta'(\Gamma)+\frac{1}{\chi_4}P_rQ\ \theta(\Gamma)+\frac{1}{\chi_a\chi_c}P_rEcf''^2(\Gamma)=0, \quad (11)$$

$$N_G=Re\left[\chi_d(1-Nr)\theta'^2+\frac{1}{\chi_a}\frac{Br}{\Omega}(f''^2+K_nf'^2)\right] \quad (12)$$

Subjected to

$$f(0)=S,f'(0)=1+\varepsilon f''(0),\ f'(\Gamma)\to 0,f'(\Gamma)\to 0,\theta'\text{as}(0)=-B_i(1-\theta(0)),\ \theta(\Gamma)\to 0,\ \Gamma\to\infty. \quad (13)$$

3 Engineering quantities of interests

The plate wall heat gradient (Nu_x) can be defined as:

$$Nu_x=\frac{xq_w}{k_f(\phi_w-\phi_\infty)}, \quad (14)$$

Using similarity variables (6), we get:

$$Nu_x Re_x^{1/2} = -\chi_d\big((1+N_r)\theta'(0)\big) \tag{15}$$

3.1. Symbols and expressions

The symbols and explanations used in the governing equation are list below:

$N_r = \frac{16}{3}\frac{\sigma^* T_\infty^3}{k^* \upsilon_f (\rho C_p)_f}$ (Thermal radiation),

$\varrho_1 = b\gamma_1$(Deborah number I),

$B_i = \frac{h_f}{k_o}\sqrt{\frac{\upsilon_f}{b}}$ (Biot number),

$\varrho_2 = b\gamma_2$(Deborah number II),

h_g (heat transfer coefficient),

μ_{thnf} (Dynamic viscosity)

$P_r = \frac{\upsilon_f}{\alpha_f}$ (Prandtl number),

$K\ \frac{\upsilon_f}{bk}$ (Porous medium),

D_1, D_2

(Velocity component),

$Nu_x \frac{x q_w}{k_f(T_w - T_\infty)}$ (local Nusselt Number),

$Re_x = \frac{U_w x}{\upsilon_f}$.(local Reynolds number),

$S = -P_w\sqrt{\frac{1}{\upsilon_f b}}$ (Suction/Injection Parameter),

k_{thnf} (Thermal conductance),

$\delta = \sqrt{\frac{b}{\mu_f}} M_w$(velocity slip).

$q_w = -k_{hnf}\frac{16}{3}\frac{\sigma^* T_\infty^3}{k^* \upsilon_f (\rho C_p)_f}\left(\frac{\partial T}{\partial y}\right)$, (heat flux),

$N_G = \frac{E_G \mu_f T_W^2}{k_f (T_w - T_\infty)^2}$ (entropy),

$Ec = \frac{U_W^2}{(C_p)_f (T_w - T_\infty)}$ (Eckert number),

$\chi_a = (1-\phi_1)^{2.5}(1-\phi_2)^{2.5}(1-\phi_3)^{2.5}(1-\phi_4)^{2.5}$, $\chi_b = \Big[(1-\phi_1)\Big\{(1-\phi_2)(1-\phi_3)\Big[(1-\phi_4) + \phi_4\left(\frac{\rho_{np4}}{\rho_{bf}}\right)\Big] + \phi_3\left(\frac{\rho_{np3}}{\rho_{bf}}\right) + \phi_2\left(\frac{\rho_{np2}}{\rho_{bf}}\right)\Big\} + \phi_1\left(\frac{\rho_{np1}}{\rho_{bf}}\right)\Big]$, $\chi_c = \Big[(1-\phi_1)\Big\{(1-\phi_2)(1-\phi_3)\Big[(1-\phi_4) + \phi_4\left(\frac{(\rho C_p)_{np4}}{(\rho C_p)_{bf}}\right)\Big] + \phi_3\left(\frac{(\rho C_p)_{np3}}{(\rho C_p)_{bf}}\right) + \phi_2\left(\frac{(\rho C_p)_{np2}}{(\rho C_p)_{bf}}\right)\Big\} + \phi_1\left(\frac{(\rho C_p)_{np1}}{(\rho C_p)_{bf}}\right)\Big]$, $\chi_d = \frac{k_{Trihnf}(k_{np4} + 2k_{Trihnf}) - 2\phi_4(k_{Trihnf} - k_{np4})}{(k_{np4} + 2k_{Trihnf}) + \phi_4(k_{Trihnf} - k_{np4})}$

4 Numerical procedures and validation test

Application of Wavelets and Chebyshev wavelets technique: Solutions to equations (5) -(8) are determined using the Wavelets and Chebyshev wavelets technique solution approach method. The solution steps are as follows:
The following simulation signifies equations (13–16) in Step 1.

$$f'''(\Gamma) + \chi_a\chi_b(ff''(\Gamma) - f'^2(\Gamma)) - \frac{1}{\omega_1}K_n f'(\Gamma) + \chi_a\chi_a(2\beta_1 f(\Gamma)f'(\Gamma)) + \beta_2 f''^2(\Gamma) + \chi_a\chi_b(\beta_1 f^2(\Gamma)f'''(\Gamma)) - \beta_2 f(\Gamma)f''^v(\Gamma) = 0, \tag{16}$$

$$\theta''(\Gamma)\left(1 + \frac{1}{\chi_d}RdPr\right) + \frac{\chi_a}{\chi_b}Prf(\Gamma)\theta'(\Gamma) - \frac{\chi_c}{\chi_a}P_r f(\Gamma)\theta'(\Gamma) + \frac{1}{\chi_4}P_r Q\ \theta(\Gamma) + \frac{1}{\chi_a\chi_c}P_r Ecf''^2(\Gamma) = 0, \tag{17}$$

Step two outlines the general form of the trial solution.

$$\emptyset(\Gamma) = \vartheta_j^p\ \sigma(\Gamma),$$

And

$$(\Gamma) = \sum_{n=1}^{2^{x-1}}\sum_{m=0}^{y-1}\Delta_{n,m}^Q \mathring{A}_{n,m}(\Gamma) = C_\iota^T \mathcal{H}(\Gamma), \mathrm{p} = j = 1,2,3,\dots 4\ for\quad \vartheta(\Gamma) = \big(\tilde{f}(\Gamma), \tilde{\theta}(\Gamma)\big) \tag{18}$$

The following provides a detailed explanation of the equations concerning the column matrices ϑ_j^p and the function $\emptyset(\Gamma)$.

$$\vartheta_\iota = \left[\Delta_{1,}^j, G\right]_j^p,\ G = 0,1,\ \dots. \tag{19}$$

Equation (20) can be restated in the following manner.

$$\tilde{\Upsilon}(\Gamma) = Æ_j^p \chi(\Gamma),\ \chi(\Gamma) = [1, \Gamma, \Gamma^2, \Gamma^3, \dots.]^p, \tag{20}$$

Step three involves generating the residuals of the equations, which include velocity thermal.

$$R_f = f'''(\Gamma) + \chi_a\chi_b(ff''(\Gamma) - f'^2(\Gamma)) - \frac{1}{\omega_1}K_n f'(\Gamma) + \chi_a\chi_a\big(2\beta_1 f(\Gamma)f'(\Gamma)\big) + \beta_2 f''^2(\Gamma) + \chi_a\chi_b\left(\beta_1 f^2(\Gamma)f'''(\Gamma)\right) - \beta_2 f(\Gamma)f''^v(\Gamma) = 0, \tag{21}$$

$$R_f = \theta''(\Gamma)\left(1 + \frac{1}{\chi_d}RdPr\right) + \frac{\chi_a}{\chi_b}Prf(\Gamma)\theta'(\Gamma) - \frac{\chi_c}{\chi_a}P_r f(\Gamma)\theta'(\Gamma) + \frac{1}{\chi_4}P_r Q\ \theta(\Gamma) + \frac{1}{\chi_a\chi_c}P_r Ecf''^2(\Gamma) = 0, \tag{22}$$

Step four. Via applying the Galerkin method, we sought to determine the unknown constants Δ's. This process resulted in the following system of nonlinear equations in a generalized form:

$$\omega_c^m = \int_0^{\Gamma_\infty} R_c \frac{O}{O\tilde{\varrho}_m^{\iota}} \tilde{c}(\Gamma), n \quad (23)$$

$$= 1, 2, .., 2^{p-1}M - 3,$$

Where $\omega_c^m = \left(Q_f^m, Q_\theta^m,\right), R_c = (R_f, R_\theta), c = (f, \theta)$,

The flow chart illustrating the numerical approach is presented in Figure 3. By substituting the appropriate unknowns, we can determine the values of Δ's. Subsequently, the values of these unknowns are ascertained.

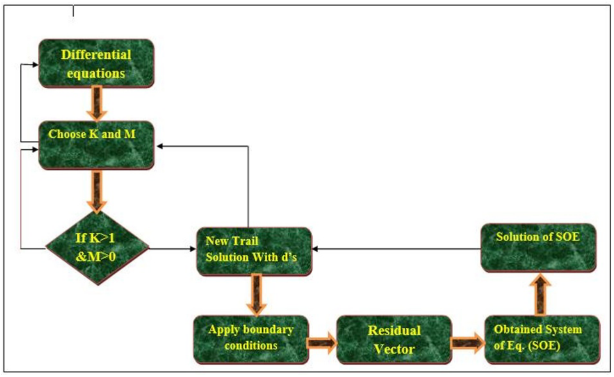

Figure 3: Flow chart utilizing wavelet method

5 Results and Discussions

The present section presents a detailed exploration of the thermal and velocity distribution through graphical, accompanied via a thorough discussion of their physical implications for different flow parameters.

Solar radiation is the process through which heat energy is transported via electromagnetic waves. The solar radiation parameter demonstrates how the transfer of heat through radiation affects the thermal distribution. The solar radiation parameter illustrates the influence of radiative heat transferal on thermal distribution (see figure 4a). When the value of the solar radiation parameter is improved, it indicates that thermal transport of thermal radiative flow has a larger effect on the thermal distribution. The NPs absorb more radiant power as the solar radiation advances, resulting in a greater thermal distribution. In reality, During the daytime, the Earth's surface transforms solar power from the Sun into heat energy via emitting solar radiation. The development adds to the elevated temperature on the Earth's surface. The fluid temperature of $SiO_2 + Ag + Cu/H_2O$ ternary nanofluid greater than the $Ag + Cu/H_2O$ hybrid nanofluid. From the result shown in Figure 4b, it is highlighted that the fluid system undergoes an irreversible process. Parameter solar radiation upsurge entropy created and such result increases more rapidly in ternary nanofluid. A rising Eckert number value shows a larger amount of kinetic energy in comparison to thermal energy. The Eckert number is vital in the field of continuum mechanics. The thermal transports are significantly boosted for Eckert number, leading to a substantial increase in the thickness of the thermal boundary layer (figure 5a). The improvement observed in $SiO_2 + Ag + Cu/H_2O$ ternary nanofluid is more significant compared to the hybrid nanofluid of $Ag + Cu/H_2O$. The influence of heat generation causes a rise in the thermal distribution, as shown in (figure 5b). The temperature inside the fluid system increases as the fluid temperature upsurges because of the exponential connection between the heat source and fluid temperature. When $SiO_2 + Ag + Cu/H_2O$ ternary nanofluid are combined with heat source, they possess the power to efficiently absorb and transform solar power into electrical energy. Figure 6a displays how β_1 impacts thermal distribution. It is crucial to highlight that a greater β_1 led to a significant increase in t thermal distribution. This upsurge occurs due to the resistance that hinders the fluid flow, causing it to slow down. The study exposed that the $SiO_2 + Ag + Cu/H_2O$ ternary nanofluid reveals higher physical properties compared to the hybrid nanofluid of $Ag + Cu/H_2O$.in order hand, the effect of β_2 reduce the thermal distribution (see Figure 6b)

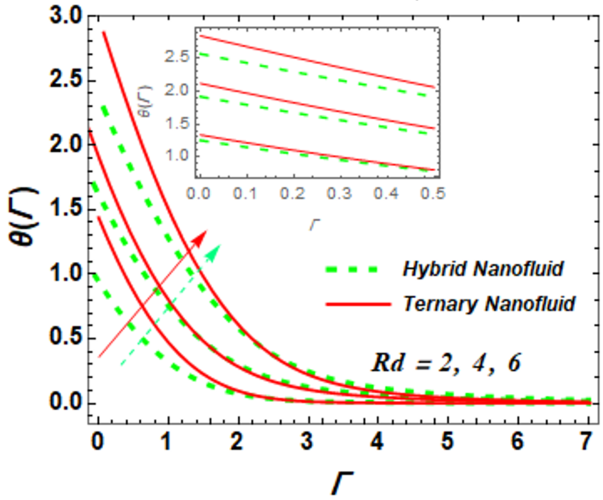

Figure 4(a). $\theta(\Gamma)$ for rising Rd.

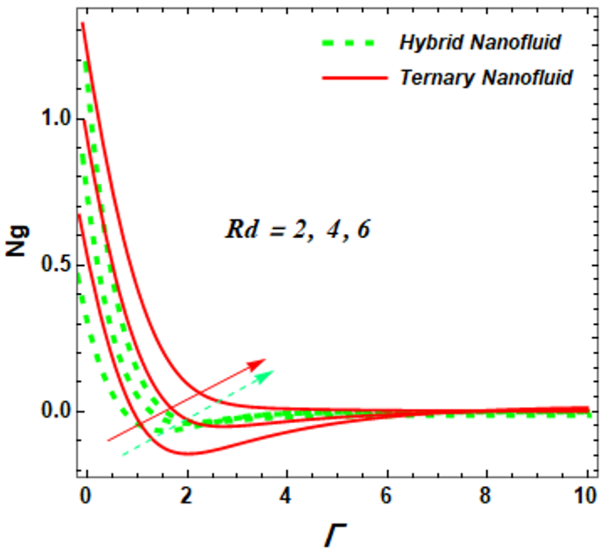

Figure 4(b). Ng for rising Rd.

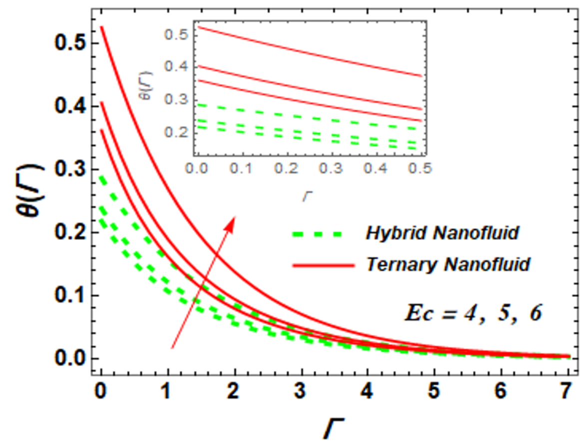

Figure 5(a). $\theta(\Gamma)$ for rising Ec.

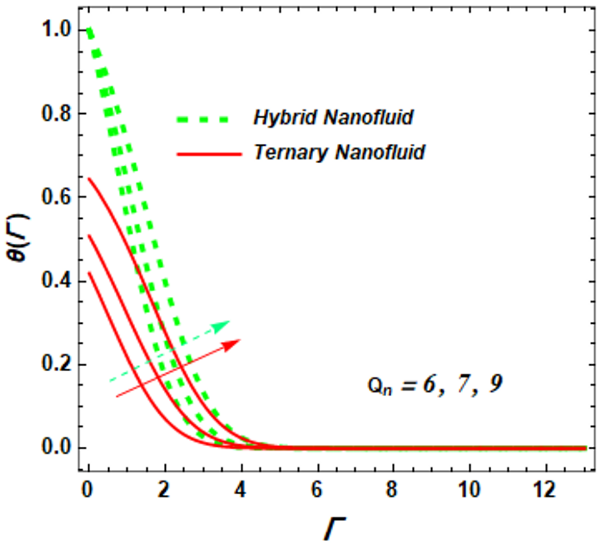

Figure 5(b). $\theta(\Gamma)$ for rising β_1.

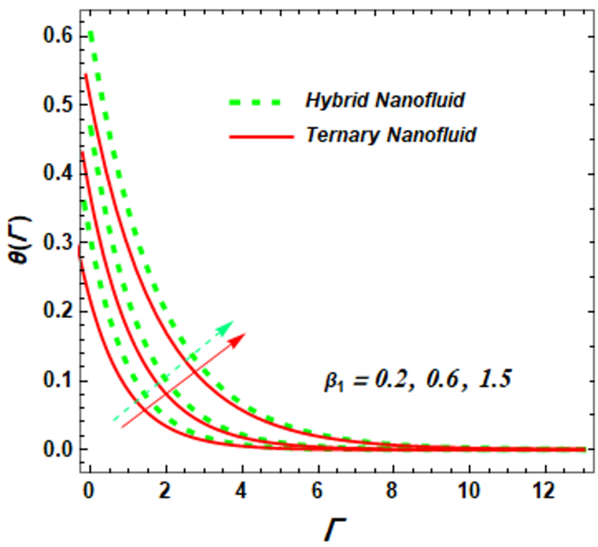

Figure 6(a). $\theta(\Gamma)$ for rising β_1.

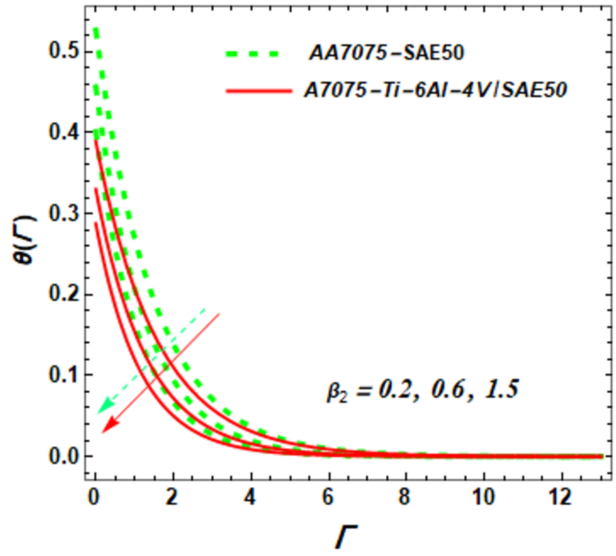

Figure 6(b). $\theta(\Gamma)$ for rising β_2.

The Deborah number is a parameter employed in the research of fluid dynamics to reveal the performance of viscoelastic substances. The fluid flow is influenced via the ratio β_1 that signifies the relationship between relaxation time and retardation time, as established in Figure 7a. When Deborah number is less than zero, it shows that the material's elasticity is higher while its viscosity is reduced. The diminution in β_2 corresponds to an improvement in viscosity compared to elasticity, as displayed in Figure 7b. The velocity distribution upsurges quickly since energy is efficiently dissipated through viscous forces. When dealing with polymer solutions with a high concentration, we might encounter elevated β_2. The injection ($S < 0$) and suction ($S > 0$) and are employed in the field of fluid mechanics to illustrate the movement of a fluid within a channel or pipe in situations where either suction or injection takes place at the wall. Figure 8a showed an increase in flow when the $S < 0$ value was less than zero. The research found that the $SiO_2 + Ag + Cu/H_2O$ ternary nanofluid had higher physical properties compared to the hybrid with $Ag + Cu/H_2O$.

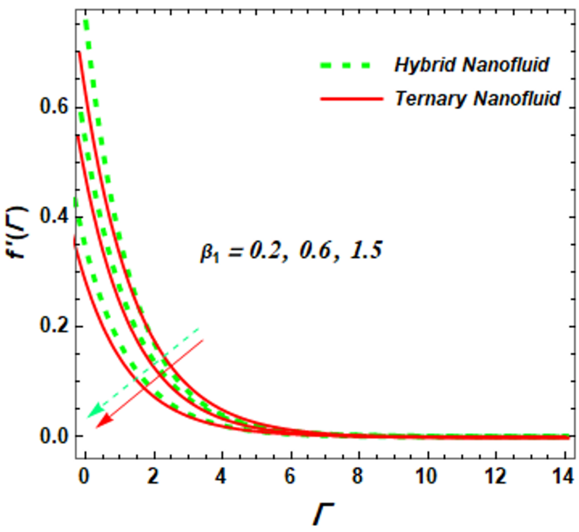

Figure 7(a). $f'(\Gamma)$ for rising β_1.

 https://doi.org/10.1051/e3sconf/202456405002

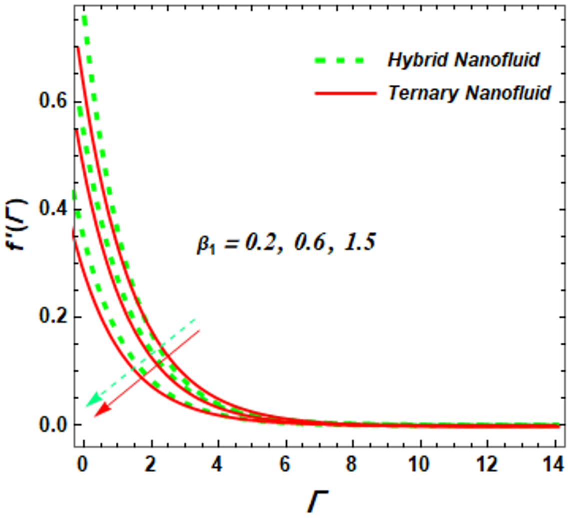

Figure 7(b). $f'(\Gamma)$ for rising β_1.

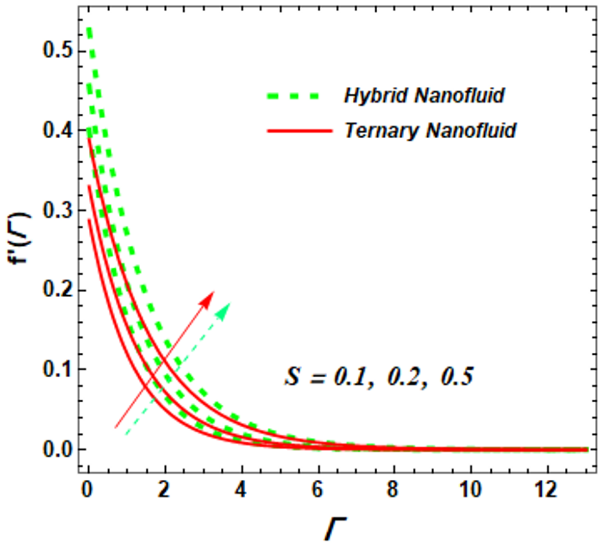

Figure 8(a). $f'(\Gamma)$ for rising $(S > 0)$.

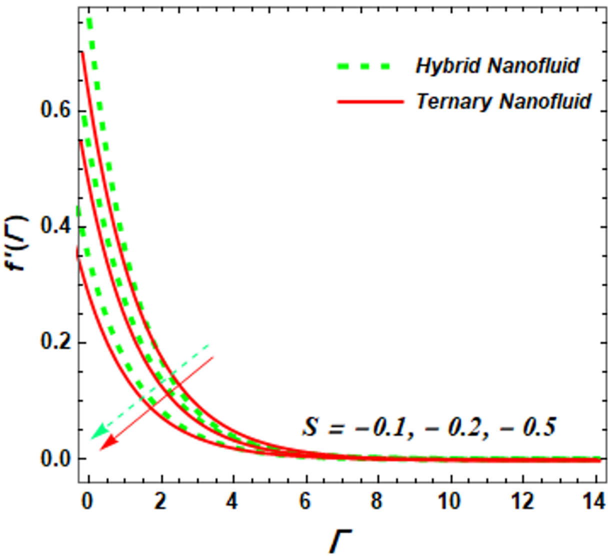

Figure 8(b). $f'(\Gamma)$ for rising $(S < 0)$.

6 Conclusion

In this paper, we conducted a study focusing on minimizing entropy production in solar energy-based water pumping systems via investigating the thermal performance of Oldryd-B-ternary nanofluid. This novel technique indicates potential to increase the usefulness and longevity of solar energy systems, thus supporting the extensive use of renewable power solutions. Hence, the following conclusions are outlined.

- Solar radiation parameter improves the field thermal field.
- The thermal distribution was enhanced via the growing value of the Deborah number and Eckert number.
- Heat transmission enhanced with mounting heat generation parameter.
- The outcomes display that the ternary nanofluid drastically boosts the thermal efficiency of the solar energy system compared to conventional fluids.
- The velocity distribution diminishes with praise of suction (S > 0).

References

1. A.M. Rashad, M.A. Nafe, D.A. Eisa, Heat generation and thermal radiation impacts on flow of magnetic Eyring-Powell hybrid nanofluid in a porous medium, Arab. J. Sci. Eng. (2022) 1–14.
2. Salawu, S. O., Yusuf, T. A., Obalalu, A. M., & Fatunmbi, E. O. (2024). Thermal radiation and propagation of tiny particles in magnetized Eyring–Powell binary reactive fluid with generalized Arrhenius kinetics. Case Studies in Thermal Engineering, 58, 104409.
3. E.O. Fatunmbi, S.S. Okoya, Quadratic mixed convection stagnation-point flow in hydromagnetic Casson nanofluid over a nonlinear stretching sheet with variable thermal conductivity, Defect Diffus. 409, 95–109.
4. Fatunmbi EO, Adigun AJ, Salawu SO. Dual stratification mechanism for nonlinear mixed convective Magneto-Tangent Hyperbolic fluid over a stretchable device with activation energy. International Journal of Applied and Computational Mathematics. 2023, ;9(4):48.J.
5. T. Rawat, J. Singh and S. Sharma, "Performance Analysis of 400 kWp Rooftop Solar Plant at Swami Keshvanand Institute of Technology, Management & Gramothan, Jaipur using PVsyst," 2023 International Conference on Power, Instrumentation, Energy and Control (PIECON), Aligarh, India, 2023, pp. 1-6, doi: 10.1109/PIECON56912.2023.10085828.
6. N. D. Waters and M. J. King, "Unsteady flow of an elastico-viscous liquid," Rheologica Acta, vol. 9, no. 3, pp. 345–355, 1970.
7. Khan, I., Imran, M., Fakhar, K. (2011). New exact solutions for an Oldroyd-B fluid in a porous medium. International Journal of Mathematics and Mathematical Sciences, 2011.
8. Oreyeni, T., Oladimeji Akindele, A., Martins Obalalu, A., Olakunle Salawu, S., Ramesh, K. (2023). Thermal

performance of radiative magnetohydrodynamic Oldroyd-B hybrid nanofluid with Cattaneo–Christov heat flux model: Solar-powered ship application. Numerical Heat Transfer, Part A: Applications, 85(12), 1954–1972. https://doi.org/10.1080/10407782.2023.2213837.

9. A. Obalalu, A. M., S. O. Salawu, M. A. Memon, O. Olayemi, M. R. Ali, R. Sadat, C. Odetunde, O. Ajala, and A. Akindele.2023. "Computational Study of Cattaneo–Christov Heat Flux on Cylindrical Surfaces Using CNT Hybrid Nanofluids: A Solar-Powered Ship Implementation."Case Studies in Ther-mal Engineering45:102959.
10. Erratum in: PLoS One. 2014;9(1) Dadheech, A., Sharma, S., Al-Mdallal, Q. Numerical simulation for MHD Oldroyd-B fluid flow with melting and slip effect. Sci Rep 14, 10591 (2024).
11. S. E. E. Hamza, MHD Flow of an Oldroyd–B Fluid through Porous Medium in a Circular Channel under the Effect of Time Dependent Pressure Gradient, American Journal of Fluid Dynamics, Vol. 7 No. 1, 2017, pp. 1-11.
12. Song, Y. Q., Farooq, A., Kamran, M., Rehman, S., Tamoor, M., Khan, R., ..., Qureshi, M. I. (2021). Analytical solution of fractional Oldroyd-B fluid via fluctuating duct. Complexity, 2021, 1-16.
13. Olayemi, O.A.; Obalalu, A.M.; Odetunde, C.B.; Ajala, O.A.: Heat transfer enhancement of magnetized nanofluid flow due toa stretch-able rotating disk with variable thermophysical properties effects.
14. Eur. Phys. J. Plus.137(3), 1–12 (2022
15. S.U.S. Choi, Enhancing thermal conductivity of fluids with nanoparticles, ASME Publ. Fed. 231 (1995) 99-106.
16. E.O. Fatunmbi et al., Analysis of hydromagnetic micropolar nanofluid flow past a nonlinear stretchable sheet and entropy generation with Navier slips, Int. J. Model. Simul. 19 (2021) 1905490.
17. A.A. Alaidrous, M.R. Eid, 3-D electromagnetic radiative non-Newtonian nanofluid flow with Joule heating and higher-order, reactions in porous materials, Sci. Rep. 10 (2020) 14513.
18. S.O. Salawu, E.O. Fatunmbi, S.S. Okoya, MHD heat and mass transport of Maxwell Arrhenius kinetic nanofluid flow over stretching surface with nonlinear variable properties, Results Chem. 3 (2021) 100125.
19. L.A. Lund, Z. Omar, I. Khan, Mathematical analysis of magnetohydrodynamic (MHD) flow of micropolar nanofluid under buoyancy effects past a vertical shrinking surface: dual solutions, Heliyon 5 (2019) e02432.
20.] S.O. Salawu, T.A. Yusuf, A.M. Obalalu, E.O. Fatunmbi. Thermal radiation and propagation of tiny particles in magnetized Eyring–Powell binary reactive fluid with generalized Arrhenius kinetics, Case Studies in Thermal Engineering 58 (2024) 104409.
21. S.U.S. Choi, Nanofluids: a new field of scientific research and innovative applications, Heat Transf. Eng. 29 (2008) 429-431.
22. Scott, T. O., Ewim, D. R., & Eloka-Eboka, A. C. (2022). Hybrid nanofluids flow and heat transfer in cavities: A technological review. International Journal of Low-Carbon Technologies, 17, 1104-1123.
23. M. Z. A. Qureshi, Q. Raza, S. M. Eldin, M. Zafar, B. Ali, I. Siddique. Thermal performance of hybrid magnetized nanofluids flow subject to joint impact of ferro oxides/CNT nanomaterials with radiative and porous factors, Case Studies in Thermal Engineering 41 (2023) 102648.
24. A. Younis, E. Elsarrag, Y. Alhorr, M. Onsa, The influence of $Al_2O_3 - ZnO - H_2O$ nanofluid on the thermodynamic performance of photovoltaic-thermal hybrid solar collector system, Innov. Ener Res. 7 (2018) 1463-2576.
25. S.K. Verma, A.K. Tiwari, S. Tiwari, D.S. Chauhan, Performance analysis of hybrid nanofluids in flat plate solar collector as an advanced working fluid, Sol. Energy.167 (2018) 231-241.
26. Adnan, K. A. M. A., Ashraf, W., Yassen, M. F., & Jamshed, W. (2023). Applied heat transfer modeling in conventional hybrid (Al2O3-CuO)/C2H6O2 and modified-hybrid nanofluids (Al2O3-CuO-Fe3O4)/C2H6O2 between slippery channel by using least square method (LSM). Future, 1, 1.
27. Mousavi SM, Esmaeilzadeh F, Wang XP. Effects of temperature and particles volume concentration on the thermophysical properties and the rheological behaviour of CuO/MgO/TiO_2 aqueous ternary hybrid nanofluid. J Therm Anal Calorim. 2019;137(3):879–901. DOI:10.1007/s10973-019-08006-0.
28. Obalalu, A. M., W. F. Alfwzan, M. A. Memon, A. Darvesh, P. Adegbite, A. S. Hendy, and M. R. Ali.2024. "Energy Optimization of Quadratic Thermal Convection on two-Phase Boundary Layer Flow Across a Moving Vertical Flat Plate."Case Studies in Thermal Engineering, 104073.
29. Obalalu, A. M., M. A. Memon, O. Olayemi, J. Olilima, and A. Fenta.2023."Enhancing Heat Transfer in Solar-Powered Ships: A Study on Hybrid Nanofluids with Carbon Nanotubes and Their Application in Parabolic Trough Solar Collectors with Electromagnetic Controls."Scientific Reports 13:9476
30. Obalalu, A. M., O. A. Olayemi, C. B. Odetunde, and O. A. Ajala.2023. "Signif-icance of Thermophoresis and Brownian Motion on a Reactive Casson-Williamson Nanofluid Past a Vertical Moving Cylinder."Computational Thermal Sciences: An International Journal15 (1).
31. H.K. Gupta, G.D. Agrawal, J. Mathur, Investigations for effect of Al2O3–H2O nanofluid flow rate on the efficiency of direct absorption solar collector, Case Stud. Therm. Eng. 5 (2015) 70–78.
32. G. Alimonti, L. Mariani, F. Prodi, R.A. Ricci, A critical assessment of extreme events trends in times of global warming, Eur. Phys. J. Plus 137 (2022) 1–20.
33. A.M. Obalalu, M. A. Memon, S. Saleem, A. Abbas, O.A. Olayemi, Mohamed R. Ali, R. Sadat, A.S. Hendy Thermal performance of Oldroyd-B hybrid nanofluid in solar energy-based water pumping systems and entropy generation minimization, Case Studies in Thermal Engineering 51 (2023) 103476.